IEEE Access
Multidisciplinary | Rapid Review | Open Access Journal

Received May 1, 2019, accepted May 16, 2019, date of publication May 28, 2019, date of current version June 13, 2019.

Digital Object Identifier 10.1109/ACCESS.2019.2919622

Ultra-Wideband 8-Port MIMO Antenna Array for 5G Metal-Frame Smartphones

XUGANG ZHANG, YIXIN LI, WEI WANG, AND WENHUI SHEN
School of Communication and Information Engineering, Shanghai University, Shanghai 200444, China
Corresponding author: Wenhui Shen (haomeni@163.com)

ABSTRACT A design of an ultra-wideband eight-port multiple-input multiple-output (MIMO) antenna array in a smartphone with an open-slot metal frame for fifth-generation (5G) communications is presented. Each element is fed by a microstrip line with a tuning stub, consisting of a U-slot on the ground plane and an open slot on the metal frame. Each slot element on the ground only occupies an area of 15 $\times$3 mm. The antenna array can operate in 3.3–6 GHz (S_{11} $<$ -6 dB) that is ultra-wide bandwidth for the future 5G communications. The antenna array is manufactured and measured. Measured antenna isolation is higher than 11 dB without any decoupling structures applied. Moreover, measured radiation patterns, antenna efficiencies, and envelop correlation coefficients are also given in this paper. High agreement between the measured and simulated results is obtained, which means that the proposed antenna is promising in engineering application.

INDEX TERMS 5G communication, metal frame, MIMO antenna, smartphone, ultra-wideband.

I. INTRODUCTION

The forthcoming of fifth generation (5G) mobile communication means higher data transfer rate. To meet the requirements, multiple-input multiple-output (MIMO) technology needs to be applied in 5G wireless communication system in that massive MIMO system can offer a high channel capacity. Conventional 2 $\times$2 MIMO antennas for long term evolution (LTE) communications can no longer afford such high data throughput, so 8 $\times$8 MIMO or even 10 $\times$10 MIMO antenna system is currently necessary [1], [2].

As a pioneer in future 5G wireless communication, sub-6 GHz spectrum of some countries is shown in Table 1 [3]. Presently, research on sub-6 GHz in most countries focuses on LTE band 42 (3400–3600 MHz) and LTE band 43 (3600–3800 MHz). Besides, 3550–4200 MHz, 3300–3400/4800–5000 MHz, and 3600–4200/4400–4900 MHz, are also included in 5G applications by the United States, China, and Japan, respectively. Furthermore, as an unlicensed band (LTE-unlicensed, LTE-U) restricted to the licensed-assisted access operation (LTE-licensed Assisted Access, LTE-LAA) [4], LTE band 46 (5150–5925 MHz) is also significant for the 5G spectrum. From the table, it is seen that different countries have allocated different sub-6 GHz bands ranging from 3.3 GHz to 6 GHz, and all these multiple licensed/unlicensed bands are going to coexist in the future 5G application. Therefore, a multi-port MIMO antenna that can continuously operate from 3.3 GHz to 6 GHz is necessary.

TABLE 1. Allocation of 5G sub-6 GHz spectrum.

Country	Band
United States	2.496–2.69 GHz, 3.55–3.7 GHz (Unlicensed), 3.7–4.2 GHz
European Union	3.4–3.8 GHz
United Kingdom	3.4–3.8 GHz
Germany	3.4–3.8 GHz
France	3.46–3.8 GHz
Italy	3.6–3.8 GHz
China	3.3–3.6 GHz, 4.8–5 GHz
South Korea	3.4–3.7 GHz
Japan	3.6–4.2 GHz, 4.4–4.9 GHz
Australia	3.4–3.7 GHz

On the other hand, the metal frame is an important component for a smartphone in industrial design. But in the meantime, it deteriorates the antenna radiation performance. Fortunately, etching open slot on the metal frame can effectively solve this problem [5], [6]. Presently, there have been some MIMO antenna designs for fourth generation (4G)

The associate editor coordinating the review of this manuscript and approving it for publication was Hassan Tariq Chattha.

2169-3536 © 2019 IEEE. Translations and content mining are permitted for academic research only.
Personal use is also permitted, but republication/redistribution requires IEEE permission.
See http://www.ieee.org/publications_standards/publications/rights/index.html for more information.

metal-frame smartphones [7]–[11]. What we need in future is 5G metal-frame-integrated MIMO antennas that support multi-band and even ultra-wideband operations.

In recent years, some MIMO antennas for 5G smartphones have been reported [12]–[30]. Regrettably, to the best of author's knowledge, designs about ultra-wideband MIMO antenna that can operate in metal-frame smartphones for 5G mobile communications are still scarce. On the one hand, some multi-mode and multi-band 5G MIMO antennas have been proposed, while few can integrate metal frame as a vital component for the smartphone. For instance, in [12], an 8-port 3.5/5.8 GHz (3400–3600/5725–5875 MHz) dual-band antenna array is formed by some inverted-F/loop antennas. A 10-antenna array with 10 T-slots can generate dual resonant modes to cover bands 42/43 and band 46 [13]. An 8-port antenna array studied in [15] also covers band 42 and band 46, using eight L-slots and eight monopoles. These exemplary multi-band antennas have shown good performances in the non-metallic smartphone platform, but their design concepts may be inapplicable in the metal-frame platform. On the other hand, it is a big challenge to design an ultra-wideband MIMO antenna array that can be integrated into 5G metal-frame smartphones. For example, an open-slot-based 8-antenna array design discussed in [16] has shown good compatibility in metal-frame smartphones. However, it only covers single LTE band 42. Another metal-frame-integrated MIMO antenna array, which consists of four identical dual-antenna building blocks, is able to cover LTE bands 41/42/43 [17]. But its working bandwidth is still not sufficient for 5G wireless communications.

Decoupling technique becomes more critical but challengeable for designing MIMO antenna, as the number of antenna element increases. Conventional decoupling technique such as neutralization line [18], [21], orthogonal modes [24], and protruded ground [31], has been applied to MIMO antenna. Recently, some different technique for MIMO antenna is reported [32]–[36]. By embedding a metamaterial polarization-rotator wall or a metasurface orthogonalize wall between two millimeter-wave (mm-wave) dielectric resonator antennas, the mutual coupling can be reduced by up to 20 dB [32]–[34]. Besides, frequency selective surface technique can also effectively reduce coupling between antennas in mm-wave MIMO system [35], [36].

Based on the above-mentioned discussions regarding the future demands and challenges of sub-6 GHz MIMO antennas, we propose an 8-port MIMO antenna array for future 5G metal-frame smartphones that can work in the frequency from 3.3 GHz to 6 GHz, which includes almost all sub-6 GHz bands in 5G applications. Each element containing a small U-slot on the ground, and a narrow slot on the metal frame, is fed by a 50-ohm microstrip line with a tuning stub. The side-edge metal frame is directly fed by the microstrip line, so part of it is exploited as the radiator to enhance the bandwidth. The proposed antenna exhibits good performance in simulated and measured results. Typical results such as S parameters, antenna efficiencies, radiation patterns, and calculated envelope correlation coefficients (ECC) are discussed in the paper.

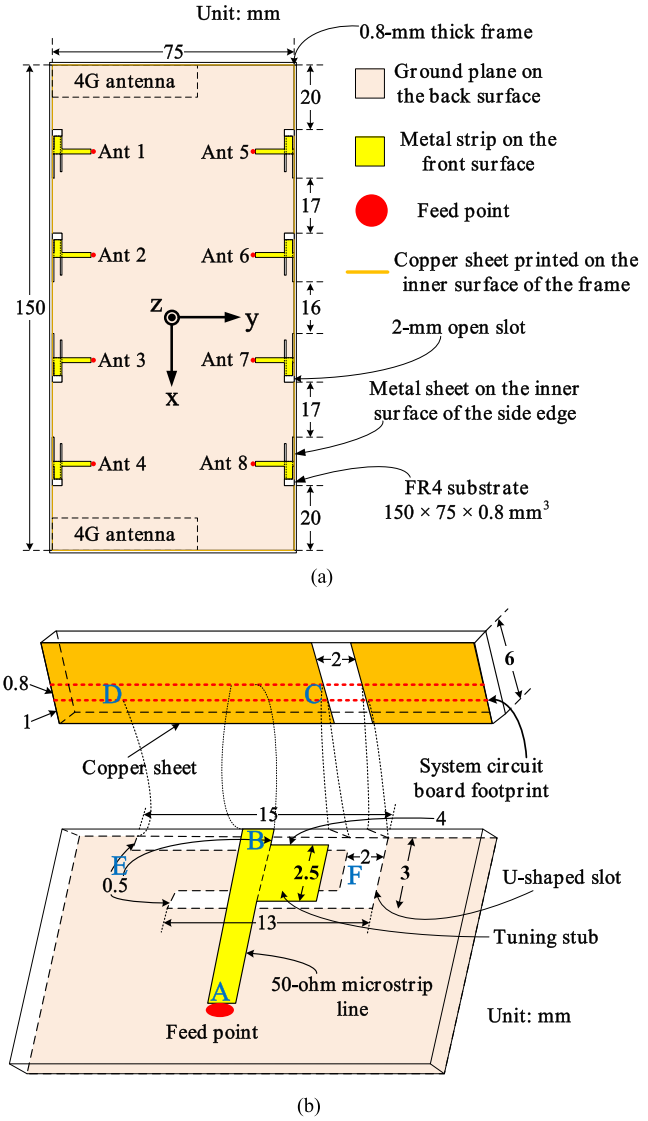

FIGURE 1. (a) Geometry of the proposed antenna array, (b) detailed structure of the antenna element.

II. PROPOSED ANTENNA ARRAY

A. ARRAY STRUCTURE

Fig. 1 shows the geometry of the proposed 8-port MIMO antenna array. An FR4 substrate with a relative permittivity of 4.4 and a loss tangent of 0.025 is used as the system circuit board (SCB) with ground plane on its back. It has a dimension of 150 mm ×75 mm ×0.8 mm. Four side-edge frames, including two long frames (left, right) and two short frames (top, bottom), are arranged perpendicularly with respect to the SCB. Copper sheets are printed on the inner surfaces of FR4 substrate, to simulate metal frames of a smartphone. All the four frames have the same height of 6 mm. They are placed 1 mm below the ground plane to accommodate the display panel.

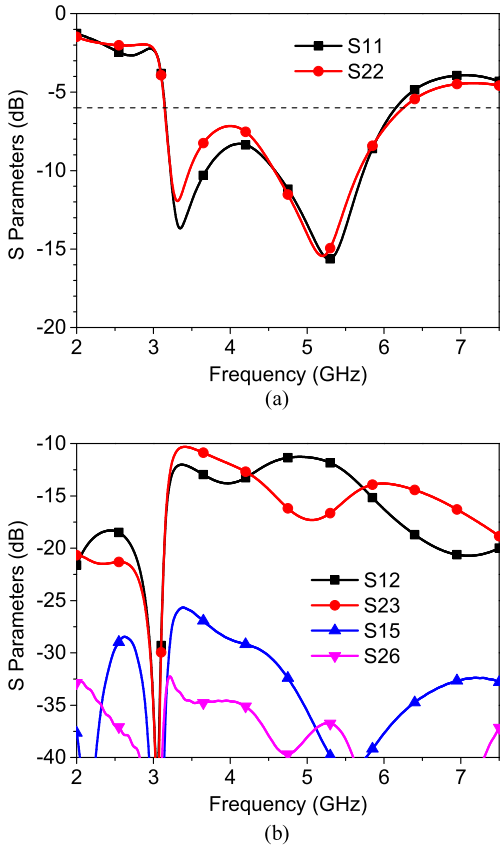

FIGURE 2. Simulated (a) reflection coefficients, (b) transmission coefficients of the proposed antenna array.

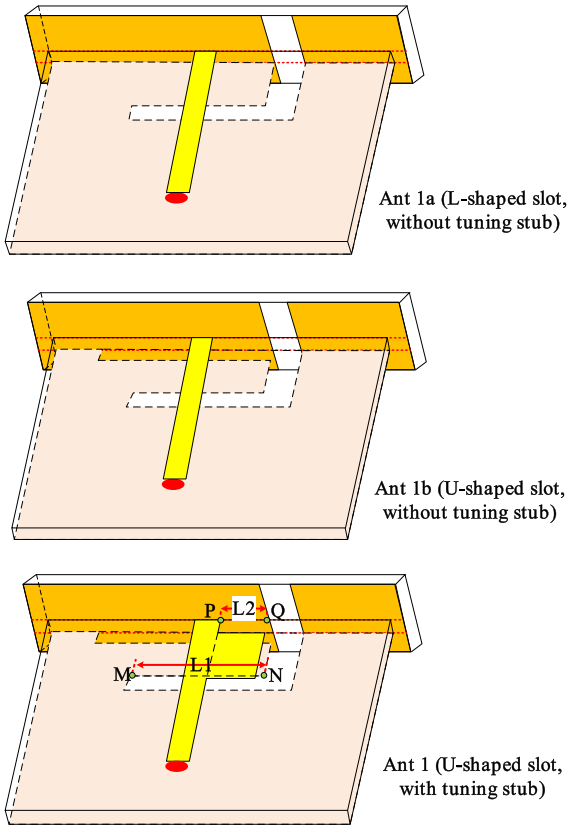

FIGURE 3. Three forms of the antenna element during the process of evolution.

As depicted in Fig. 1(a), eight identical antennas (Ants 1–8) are disposed at the long side of the SCB. In order to reserve enough space for 4G antennas, the elements at the top and bottom i.e., Ant 1, Ant 4, Ant 5 and Ant 8, are 20 mm away from the metal frame. All antennas are symmetrical about the center of the SCB, details can be seen in the figure.

B. ANTENNA ELEMENT

The detailed structure of the antenna element is illustrated in Fig. 1(b). The 50-ohm microstrip line with a rectangular tuning stub is used to feed the antenna element. A 0.5-mm wide U-slot, whose one arm is 15 mm long and the other one is 13 mm long, is etched on the ground plane. The U-slot is of 15 mm $\times$3 mm large. A 2-mm wide slot on the metal frame joins with the U-slot. The feed strip is electrically connected to the side-edge metal frame. Each antenna element consists of three parts: the feed strip (section AB), part of the metal frame (section CD), and part of the ground (section EF). The antenna element has a maximum length of 13 mm, which is still less than a quarter of wavelength, even though the metal frame is a part of the antenna structure. Detailed working principle will be introduced in section III of the article.

III. DESIGN PROCESS

Simulated S parameters of the elements are depicted in Fig. 2. Because of the centrosymmetric structure of the proposed antenna array, the eight antenna elements can be divided into two parts, i.e. Ant 1, Ant 4, Ant 5 and Ant 8 belong to one category and the other four antennas belong to the other category. So, we can assume that $S_{11} = S_{44} = S_{55} = S_{88}$, and $S_{22} = S_{33} = S_{66} = S_{77}$. Thus, only reflection coefficients of Ant 1 and Ant 2 are given in Fig. 2(a). As can be seen in Fig. 2(a), the antenna element can cover bandwidth of 3.3–6 GHz, which contains most sub-6-GHz bands. As for the isolations, there are also $S_{12} = S_{34} = S_{56} = S_{78}$, $S_{23} = S_{67}$, $S_{15} = S_{48}$, and $S_{26} = S_{37}$. As shown in Fig. 2(b), all isolations are higher than 10 dB. Among which S_{15} and S_{26} are higher compared to S_{12} and S_{23}, because Ants 1, 5 and Ants 2, 6 are oppositely placed.

The procedure of element design is shown in Fig. 3. Ant 1a is fed by a microstrip line with an L-slot underneath. In Ant 1b, a new branch slot is etched, thus the L-slot becomes a U-slot, leading to a new resonance at 3.6 GHz. As for Ant 1, a rectangular tuning stub is added on the right side of the feed line, leading to wider impedance bandwidth of 3.3–6 GHz, which is the targeted 5G band in sub-6 GHz spectrum. Details can be seen in Fig. 4 and Table 2.

The variation of S_{11} with different values of L1 and L2 is shown in Fig. 5. It can be clearly seen that the lengths of L1 and L2 affect the resonance of low frequency and high frequency, respectively, which means that the proposed antenna element can be independently adjusted, even though

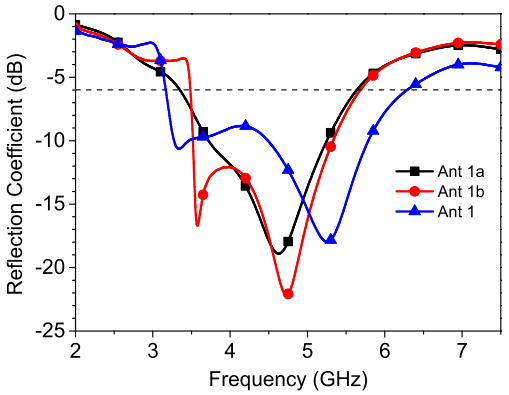

FIGURE 4. Reflection coefficients of Ant 1a, Ant 1b, and Ant 1.

TABLE 2. Evolution of the antenna element.

Name	Bandwidth (GHz)	Number of Resonance
Ant 1a	3.35–5.64	1
Ant 1b	3.48–5.68	2
Ant 1	3.16–6.28	2

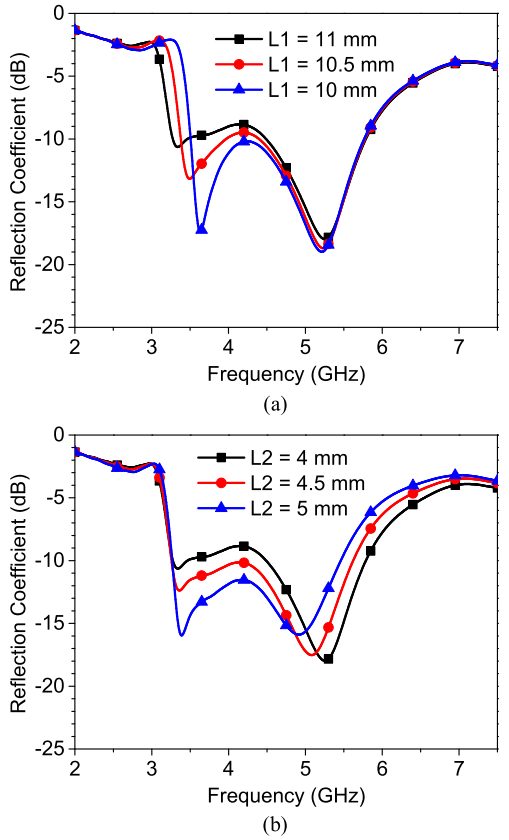

FIGURE 5. Reflection coefficients of Ant 1 with different values of (a) L1, (b) L2.

it supports a very wide bandwidth of sub-6 GHz. This unique characteristic makes it easy to be operated in engineering application. The simulated surface current distributions at the two resonances are demonstrated in Fig. 6. To demonstrate the current on the ground clearly, the feed strip is not shown in Fig. 6(a). It is clear to see that the current concentrates on path ABDEF at 3.3 GHz. When the antenna resonances at 5.3 GHz, the current mainly concentrates on path ABC. This result verifies the characteristic obtained from Fig. 5, indicating that part of the ground and part of the metal frame are used as the radiators of the antenna. Essentially, each antenna element can be considered as an asymmetrical dipole.

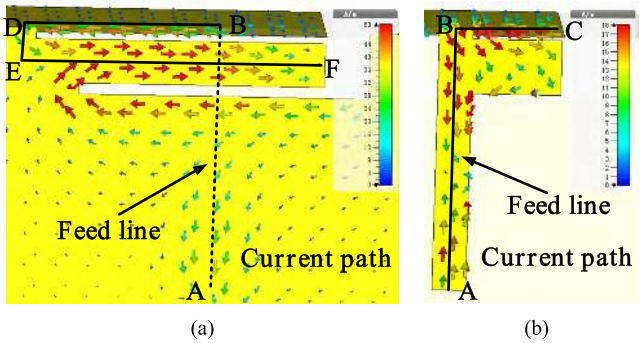

FIGURE 6. Surface current distributions of the antenna element at (a) 3.3 GHz, (b) 5.3 GHz.

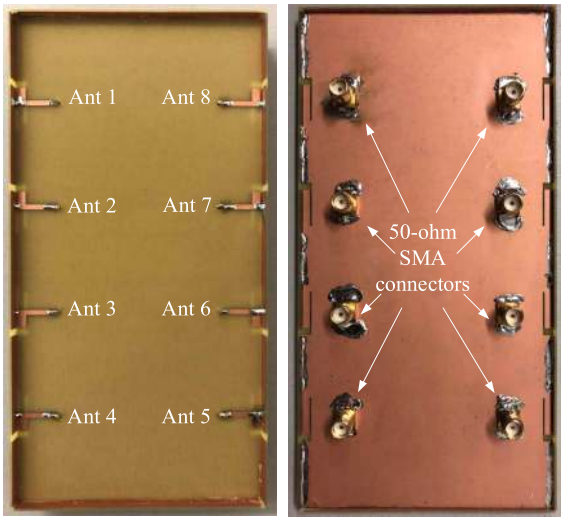

FIGURE 7. Photos of the fabricated antenna array.

IV. RESULTS AND DISCUSSION

A. S PARAMETERS

The proposed 8-port MIMO antenna array was fabricated and measured, and its front and back view is demonstrated in Fig. 7. Each element was connected to a 50-ohm SMA connector. Their S parameters were measured by an Agilent vector network analyzer. The measured S parameters shown in Fig. 8 are agree with those simulated ones shown in Fig. 2. Owing to the symmetrical structure, only the reflection coefficients of Ants 1–4 are given in Fig. 8(a). The measured S_{11}, S_{22}, S_{33}, and S_{44} are smaller than -6 dB between 3.3 GHz and 6 GHz, and the measured transmission coefficients (S_{21}, S_{32},

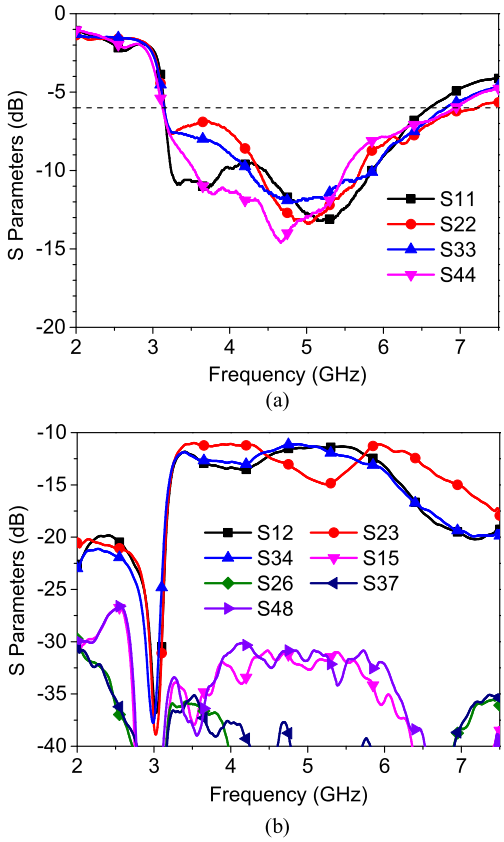

FIGURE 8. Measured (a) reflection coefficients, (b) transmission coefficients of the fabricated antenna array.

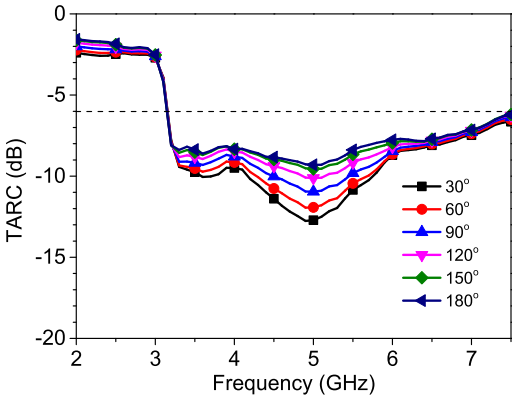

FIGURE 9. Simulated and measured antenna efficiencies of Ant 1, Ant 2, Ant 3, and Ant 4.

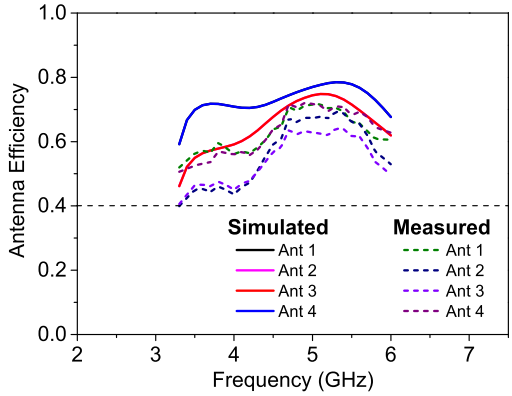

FIGURE 10. Simulated and measured antenna efficiencies of Ant 1, Ant 2, Ant 3, and Ant 4.

and S_{43}) are all less than -10 dB within the desired frequency band. -6dB bandwidth is generally acceptable for an antenna working in sub-6 GHz bands. The isolations between nonadjacent antennas are much higher than those between adjacent antennas, so they are not plotted in the figure. The measured S parameters indicate that the proposed 8-port MIMO antenna array can cover all 5G sub-6 GHz bands effectively.

To further validate the effective bandwidth of the antenna array, total active reflection coefficients (TARC) are calculated using the measured S parameters. The amplitude of all excitations is kept the same while the excitation phases vary with respect to port 1 [37], [38]. The TARC curves for different excitation phases are depicted in Fig. 9. It can be seen that the -6dB bandwidth of the proposed antenna array can always covers 3.3-6 GHz with excitation phases varying.

B. RADIATION PERFORMANCES

The radiation performances of the proposed antenna array were tested in a microwave anechoic chamber. Fig. 10 shows the simulated and measured total efficiencies of Ants 1–4, with solid lines representing for simulated results, and dash lines for measured results. It can be seen that simulated result of Ant 1 coincides with that of Ant 4, and simulated result of Ant 2 coincides with that of Ant 3. The measured antenna efficiencies of Ant 1 and Ant 4 are about 3%–12% higher than those of Ant 2 and Ant 3. This is possibly because Ants 1 and 4 have lower coupling losses. All measured antenna efficiencies are about 40%–71% within the entire bandwidth, which are 5%–16% lower than the simulated antenna efficiencies. Nevertheless, the measured results are still acceptable for the 5G MIMO applications.

The radiation patterns in xy-plane and yz-plane of Ant 1 and Ant 2 at 3.5 GHz, 4 GHz, 4.9 GHz, and 5.5 GHz are plotted in Fig. 11 and Fig. 12, respectively. As for the rest of the antenna elements, the radiation patterns are not shown for brevity. As illustrated in Fig. 11, the co-polarization component (E-phi) shows agreement with the simulated one. Both Ant 1 and Ant 2 exhibit almost omnidirectional radiations in xy-plane, and the radiation in -y direction is a little stronger, which is the external direction of the SCB. Similarly, except Ant 2 at 5.5 GHz, omnidirectional radiations of Ant 1 and Ant 2 in yz-plane are observed from Fig. 12, which are important in a smartphone. These results mean that all antenna elements show good radiation characteristics at the four representative frequencies (ranging from sub-6 GHz low band to sub-6 GHz high band), even though the proposed antenna array covers ultra-wide bandwidth, indicating that the

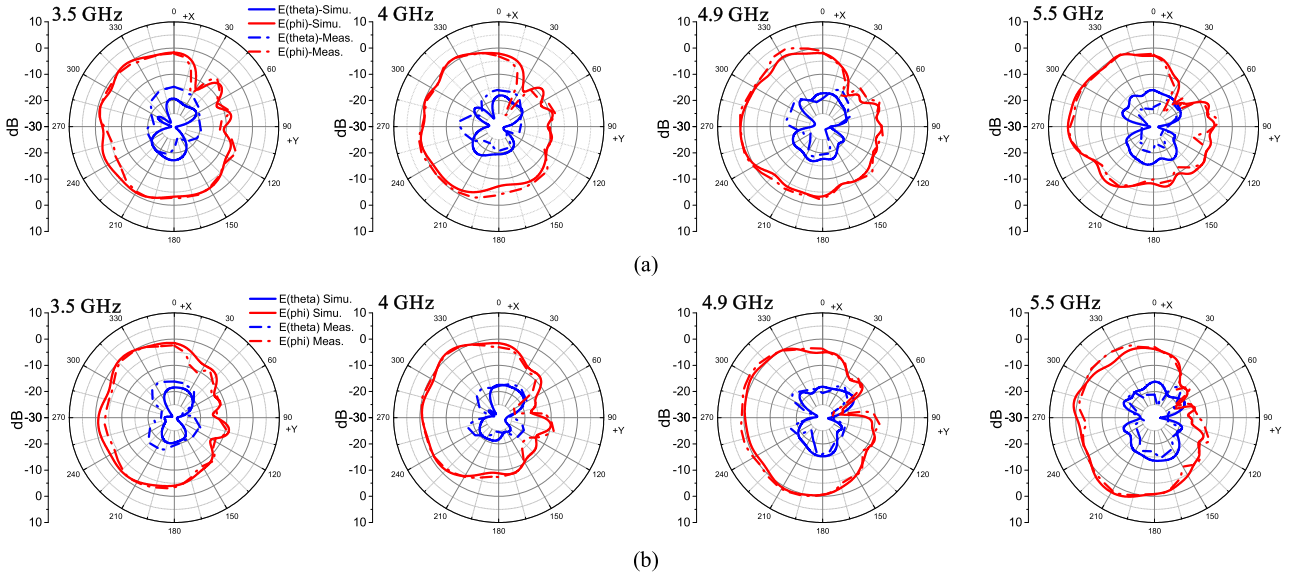

FIGURE 11. Simulated and measured radiation patterns in xy-plane of (a) Ant 1, (b) Ant 2 at 3.5 GHz, 4 GHz, 4.9 GHz, and 5.5 GHz within the operating band.

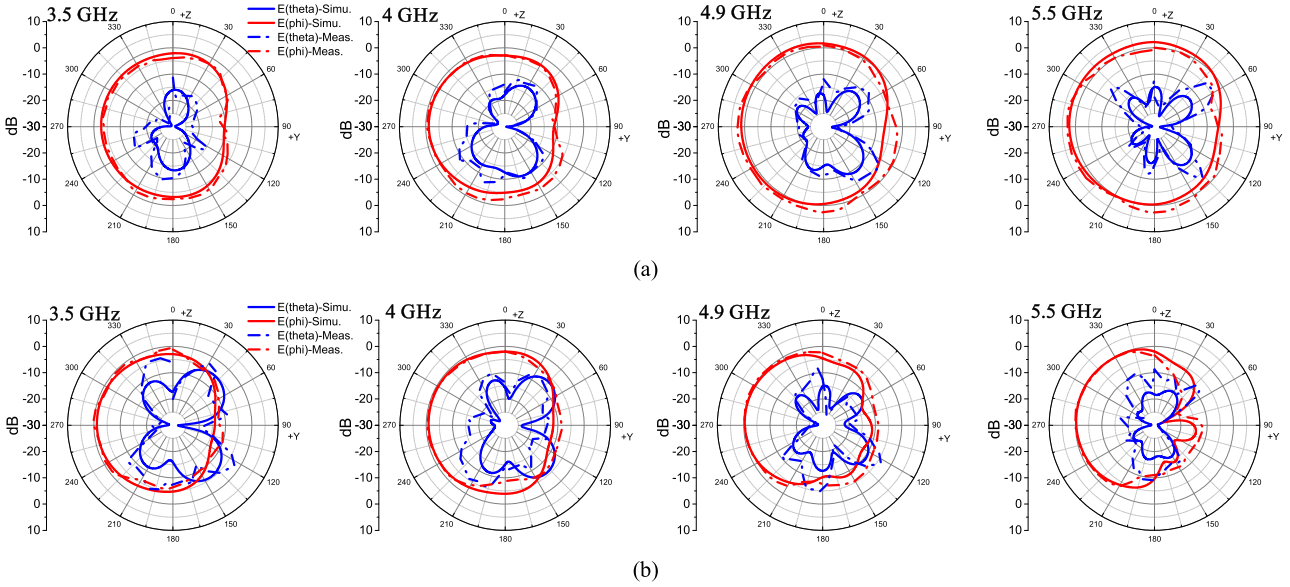

FIGURE 12. Simulated and measured radiation patterns in yz-plane of (a) Ant 1, (b) Ant 2 at 3.5 GHz, 4 GHz, 4.9 GHz, and 5.5 GHz within the operating band.

proposed antenna array has promising radiation performance in mobile communication applications.

C. MIMO PERFORMANCES

Another important factor to evaluate the diversity and multiplexing of MIMO antennas is ECC. The simulated and measured ECC values between Ant 1 and Ant 2, Ant 2 and Ant 3, Ant 3 and Ant 4, Ant 1 and Ant 5 are given in Fig. 13. The measured ECCs are computed from measured complex electric field results. In simulation, the maximum ECC is 0.12, which is between Ant 2 and Ant 3. ECCs between another adjacent antenna elements are less than 0.05, as shown in Fig. 13(a). In addition, it can be clearly observed that all measured ECCs are no more than 0.09 within the operating frequency band. The low ECCs suggest that the proposed 8-port antenna array exhibits desirable MIMO diversity performance for 5G system.

The ergodic channel capacity of the fabricated antenna array is calculated, by assuming the MIMO system is in an independent and identically distributed Rayleigh fading environment with SNR of 20 dB. As displayed in Fig. 14, the calculated channel capacity of the proposed antenna array is about 35–40 bps/Hz. In contrast, a 2 $\times$2 MIMO system can only reach a maximum channel capacity of 11.5 bps/Hz.

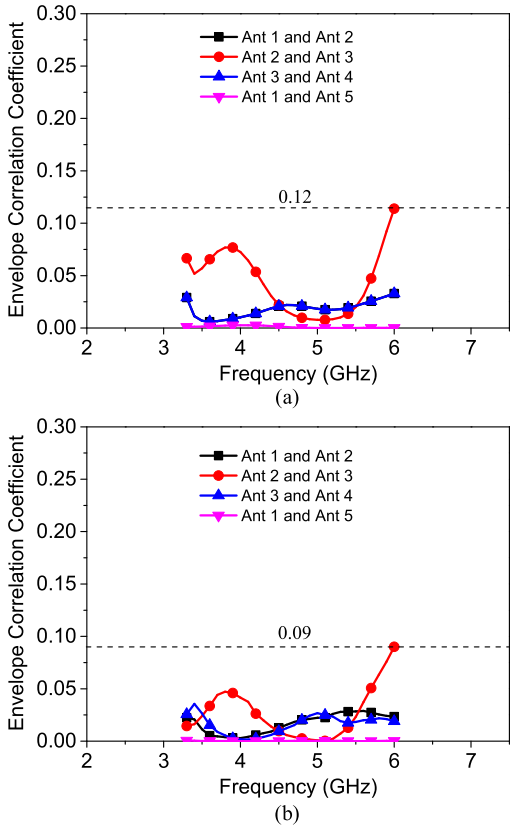

FIGURE 13. (a) Simulated and (b) measured ECCs between some adjacent antenna elements.

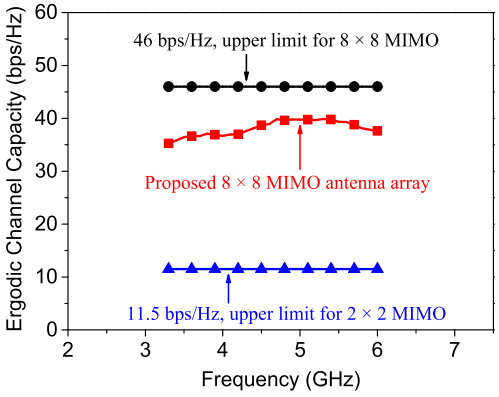

FIGURE 14. Calculated ergodic channel capacity of the proposed 8 ×8 MIMO antenna array.

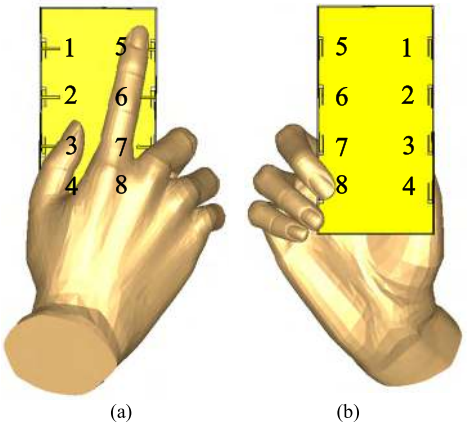

FIGURE 15. Antenna array with single-hand holding: (a) front side, (b) back side.

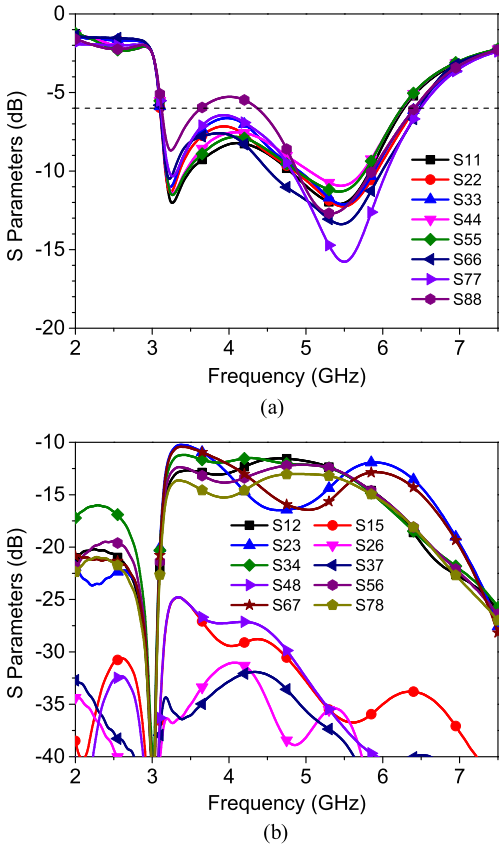

FIGURE 16. Simulated (a) reflection coefficients, (b) isolations of the antenna array in the circumstance of single-hand holding.

Therefore, the 8 ×8 MIMO scheme has an advantage in data throughput compared to 2 ×2 MIMO scheme.

D. EFFECTS OF HAND

The effect of user's hand for the proposed antenna array is also investigated in this section. As shown in Fig. 15, the antenna array is held by a hand. The simulated S parameters with handing are plotted in Fig. 16. It can be seen in Fig. 16(a) that all antenna elements except Ant 8 can still cover 3.3–6 GHz. The performance of Ant 8 is deteriorated, because it is almost entirely covered by the middle finger. It is demonstrated in Fig. 16(b) that all isolations between adjacent antenna elements are still higher than 10 dB.

The simulated total efficiencies of the eight antennas are depicted in Fig. 17. Note that the efficiencies of Ants 1–5 are almost unchanged, but those of Ants 6–8 become lower than 40% compared to the free space circumstance. This is because the hand is a lossy medium which will absorb electromagnetic radiation energy, causing the deterioration

TABLE 3. Comparison between the proposed 5G MIMO antenna and others.

Reference	Metal Frame	Effective Bandwidth (GHz)	Total Efficiency (%)	Isolation (dB)	ECC	Peak Channel Capacity (bps/Hz, 20-dB SNR)
Proposed	**Yes**	**3.3–4.2 (–6 dB), 4.4–5 (–6 dB), 5.15–5.925 (–6 dB)**	**40–71**	**> 11**	**< 0.1**	**40 (8 × 8 MIMO)**
[12]	No	3.4–3.6 (–6 dB), 5.725–5.875 (–6 dB)	48–80	> 10	< 0.15	42 (8 × 8 MIMO)
[13]	No	3.4–3.8 (–6 dB), 5.15–5.925 (–6 dB)	42–82	> 11	< 0.15	51.4 (10 × 10 MIMO)
[14]	No	3.4–3.8 (–6 dB), 5.15–5.925 (–6 dB)	41–82	>12	< 0.15	37 (8 × 8 MIMO) 29.5 (6 × 6 MIMO)
[15]	No	3.4–3.6 (–10 dB), 5.15–5.925 (–6 dB)	50–68	> 12	< 0.1	40 (8 × 8 MIMO)
[16]	Yes	3.4–3.6 (–6 dB)	45–60	> 12	< 0.1	37 (8 × 8 MIMO)
[17]	Yes	2.496–2.69 (–6 dB), 3.4–3.8 (–6 dB)	44–66	> 10.5	< 0.2	38.3 (8 × 8 MIMO)
[18]	No	3.4–3.6 (–6 dB)	40–60	> 10	< 0.25	38 (8 × 8 MIMO)
[20]	No	3.4–3.6 (–6 dB)	55–59	> 10	Not mentioned	16 (2 × 8 MIMO)
[21]	No	3.4–3.6 (–10 dB)	62–78	> 10	< 0.2	40 (8 × 8 MIMO)
[22]	No	3.4–3.8 (–6 dB)	42–62	> 10	< 0.1	47 (10 × 10 MIMO)
[25]	No	2.55–2.65 (–10 dB)	48–63	> 12.5	< 0.15	40 (8 × 8 MIMO)
[27]	No	3.4–3.6 (–6 dB)	40–52	> 10	< 0.15	35 (8 × 8 MIMO)
[29]	No	3.4–3.8 (–6 dB), 5.15–5.925 (–6 dB)	49–75	> 11	< 0.1	43.3 (8 × 10 MIMO)
[30]	No	3.4–3.6 (–6 dB), 4.8–5.1 (–6 dB)	40–85	> 11.5	< 0.1	38.5 (8 × 8 MIMO)

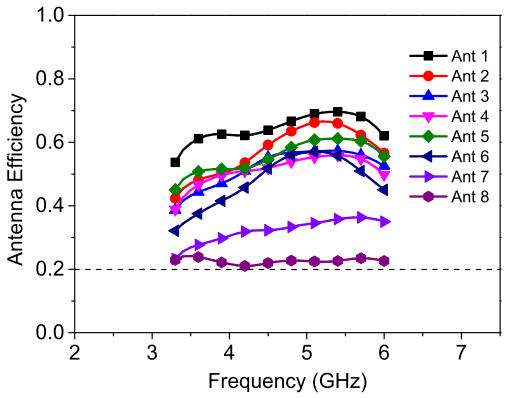

FIGURE 17. Simulated antenna efficiencies in the circumstance of single-hand holding.

of antenna efficiencies. However, all simulated total efficiencies are still higher than 20%, which are acceptable for 5G smartphone MIMO system with the hand presence.

In addition, a comparison between the proposed MIMO antenna and some other MIMO antennas in references is listed in Table 3. As can be seen, most referenced antennas cannot be integrated into metal-frame smartphones, which may not meet the industrial demand. Furthermore, the proposed MIMO antenna array has wider bandwidth than all the other MIMO antenna arrays listed in this table. The ECCs of the proposed work are also relatively low. In addition, compared to the 8-port MIMO antennas introduced in [14], [16]–[18], [27] and [30], the proposed MIMO antenna array has a higher peak channel capacity.

V. CONCLUSION

In this paper, an ultra-wideband 8-port MIMO antenna array for 5G applications is designed, manufactured, and tested. Using a part of metal frame as a radiation branch, the antenna array can work properly in a metal-frame smartphone. The measured results show that the working frequency band of the proposed antenna array is able to cover 3.3–6 GHz, with isolation higher than 11 dB. The measured antenna efficiencies are higher than 40% within the operating bandwidth. The calculated ECCs from measured E-field results are less than 0.09, and the calculated channel capacity is between 35 bps/Hz and 40 bps/Hz with 20-dB SNR. In the handheld circumstance, at least seven antenna elements have desirable radiation performances (reflection coefficients < –6 dB, total efficiency > 20%) within 3.3–6 GHz. All results indicate that the proposed MIMO antenna array is a good candidate for the forthcoming 5G massive MIMO mobile communication systems.

REFERENCES

[1] A. Al-Dulaimi, S. Al-Rubaye, Q. Ni, and E. Sousa, "5G communications race: Pursuit of more capacity triggers LTE in unlicensed band," *IEEE Veh. Technol. Mag.*, vol. 10, no. 1, pp. 43–51, Mar. 2015.
[2] M. Agiwal, A. Roy, and N. Saxena, "Next generation 5G wireless networks: A comprehensive survey," *IEEE Commun. Surveys Tuts.*, vol. 18, no. 3, pp. 1617–1655, 3rd Quart., 2016.
[3] Qualcomm. *What Can We Do With 5G NR Spectrum That Isn't Possible Today?*. Accessed: Dec. 13, 2017. [Online]. Available: https://www.qualcomm.com/media/documents/files/new-3gpp-effort-on-nr-in-unlicensed-spectrum-expands-5g-to-new-areas.pdf
[4] H. Xu, H. Wang, S. Gao, H. Zhou, Y. Huang, Q. Xu, and Y. Cheng, "A compact and low-profile loop antenna with six resonant modes for LTE smartphone," *IEEE Trans. Antennas Propag.*, vol. 64, no. 9, pp. 3743–3751, Sep. 2016.

[5] D. Huang and Z. Du, "Eight-band antenna with a small ground clearance for LTE metal-frame mobile phone applications," *IEEE Antennas Wireless Propag. Lett.*, vol. 17, no. 1, pp. 34–37, Jan. 2018.

[6] S.-C. Chen, C.-C. Huang, and W.-S. Cai, "Integration of a low-profile, long-term evolution/wireless wide area network monopole antenna into the metal frame of tablet computers," *IEEE Trans. Antennas Propag.*, vol. 65, no. 7, pp. 3726–3731, Jul. 2017.

[7] H. D. Chen, H. W. Yang, and C. Y. D. Sim, "Single open-slot antenna for LTE/WWAN smartphone application," *IEEE Trans. Antennas Propag.*, vol. 65, no. 8, pp. 4278–4282, Aug. 2017.

[8] Y. Yang, Z. Zhao, W. Yang, Z. Nie, and Q.-H. Liu, "Compact multimode monopole antenna for metal-rimmed mobile phones," *IEEE Trans. Antennas Propag.*, vol. 65, no. 5, pp. 2297–2304, May 2017.

[9] Y. L. Ban, Y. F. Qiang, Z. Chen, K. Kang, and J. H. Guo, "A dual-loop antenna design for hepta-band WWAN/LTE metal-rimmed smartphone applications," *IEEE Trans. Antennas Propag.*, vol. 63, no. 1, pp. 48–58, Jan. 2015.

[10] Y.-H. Zhang, S.-R. Yang, Y.-L. Ban, Y.-F. Qiang, J. Guo, and Z.-F. Yu, "Four-feed reconfigurable MIMO antenna for metal-frame smartphone applications," *IET Microw., Antennas Propag.*, vol. 12, no. 9, pp. 1477–1482, Jul. 2018.

[11] Z.-Q. Xu, Y. Sun, Q.-Q. Zhou, Y.-L. Ban, Y.-X. Li, and S. S. Ang, "Reconfigurable MIMO antenna for integrated-metal-rimmed smartphone applications," *IEEE Access*, vol. 5, pp. 21223–21228, 2017.

[12] K.-L. Wong, B.-W. Lin, and B. W.-Y. Li, "Dual-band dual inverted-F/loop antennas as a compact decoupled building block for forming eight 3.5/5.8-GHz MIMO antennas in the future smartphone," *Microw. Opt. Technol. Lett.*, vol. 59, no. 11, pp. 2715–2721, Nov. 2017.

[13] Y. Li, C.-Y.-D. Sim, Y. Luo, and G. Yang, "Multiband 10-antenna array for sub-6 GHz MIMO applications in 5-G smartphones," *IEEE Access*, vol. 6, pp. 28041–28053, 2018.

[14] Y. Li, C.-Y.-D. Sim, Y. Luo, and G. Yang, "12-port 5G massive MIMO antenna array in sub-6GHz mobile handset for LTE bands 42/43/46 applications," *IEEE Access*, vol. 6, pp. 344–354, 2018.

[15] H. Zou, Y. Li, C.-Y.-D. Sim, and G. Yang, "Design of 8 × 8 dual-band MIMO antenna array for 5G smartphone applications," *Int. J. RF Microw. Comput. Aided Eng.*, vol. 28, no. 9, Nov. 2018, Art. no. e21420.

[16] J.-Y. Lu, K.-L. Wong, and W.-Y. Li, "Compact eight-antenna array in the smartphone for the 3.5-GHz LTE 8 × 8 MIMO operation," in *Proc. IEEE Asia–Pacific Conf. Antennas Propag.*, Kaohsiung, Taiwan, Jul. 2016, pp. 323–324.

[17] Y. Li, C.-Y.-D. Sim, Y. Luo, and G. Yang, "Metal-frame-integrated eight-element multiple-input multiple-output antenna array in the long term evolution bands 41/42/43 for fifth generation smartphones," *Int. J. RF Microw. Comput. Aided Eng.*, vol. 29, no. 1, Jan. 2019, Art. no. e21495.

[18] K.-L. Wong, J.-Y. Lu, L.-Y. Chen, W.-Y. Li, and Y.-L. Ban, "8-antenna and 16-antenna arrays using the quad-antenna linear array as a building block for the 3.5-GHz LTE MIMO operation in the smartphone," *Microw. Opt. Technol. Lett.*, vol. 58, no. 1, pp. 174–181, Jan. 2016.

[19] Q. Chen, H. Lin, J. Wang, L. Ge, Y. Li, T. Pei, and C.-Y.-D. Sim, "Single ring slot-based antennas for metal-rimmed 4G/5G smartphones," *IEEE Trans. Antennas Propag.*, vol. 67, no. 3, pp. 1476–1487, Mar. 2019.

[20] A. A. Al-Hadi, J. Ilvonen, R. Valkonen, and V. Viikari, "Eight-element antenna array for diversity and mimo mobile terminal in LTE 3500 MHz band," *Microw. Opt. Technol. Lett.*, vol. 56, no. 6, pp. 1323–1327, Jun. 2014.

[21] Y.-L. Ban, C. Li, C.-Y.-D. Sim, G. Wu, and K.-L. Wong, "4G/5G multiple antennas for future multi-mode smartphone applications," *IEEE Access*, vol. 4, pp. 2981–2988, 2016.

[22] K.-L. Wong and J. Y. Lu, "3.6-GHz 10-antenna array for mimo operation in the smartphone," *Microw. Opt. Technol. Lett.*, vol. 57, no. 7, pp. 1699–1704, Jul. 2015.

[23] M.-Y. Li, Y.-L. Ban, Z.-Q. Xu, J. Guo, and Z.-F. Yu, "Tri-polarized 12-antenna MIMO array for future 5G smartphone applications," *IEEE Access*, vol. 6, pp. 6160–6170, Dec. 2017.

[24] L. Sun, H. Feng, Y. Li, and Z. Zhang, "Compact 5G MIMO mobile phone antennas with tightly arranged orthogonal-mode pairs," *IEEE Trans. Antennas Propag.*, vol. 66, no. 11, pp. 6364–6369, Nov. 2018.

[25] M.-Y. Li, Y.-L. Ban, Z.-Q. Xu, G. Wu, C.-Y.-D. Sim, K. Kang, and Z.-F. Yu, "Eight-port orthogonally dual-polarized antenna array for 5G smartphone applications," *IEEE Trans. Antennas Propag.*, vol. 64, no. 9, pp. 3820–3830, Sep. 2016.

[26] A. Zhao and Z. Ren, "Size reduction of self-isolated MIMO antenna system for 5G mobile phone applications," *IEEE Antennas Wireless Propag. Lett.*, vol. 18, no. 1, pp. 152–156, Jan. 2019. doi: 10.1109/LAWP.2018.2883428.

[27] K.-L. Wong, C.-Y. Tsai, and J.-Y. Lu, "Two asymmetrically mirrored gap-coupled loop antennas as a compact building block for eight-antenna MIMO array in the future smartphone," *IEEE Trans. Antennas Propag.*, vol. 65, no. 4, pp. 1765–1778, Apr. 2017.

[28] H. Xu, H. Zhou, S. Gao, H. Wang, and Y. Cheng, "Multimode decoupling technique with independent tuning characteristic for mobile terminals," *IEEE Trans. Antennas Propag.*, vol. 65, no. 12, pp. 6739–6751, Dec. 2017.

[29] Y. Li and G. Yang, "Dual-mode and triple-band 10-antenna handset array and its multiple-input multiple-output performance evaluation in 5G," *Int. J. RF Microw. Comput. Aided Eng.*, vol. 29, no. 2, Feb. 2019, Art. no. e21538.

[30] J. L. Guo, L. Cui, C. Li, and B. H. Sun, "Side-edge frame printed eight-port dual-band antenna array for 5G smartphone applications," *IEEE Trans. Antennas Propag.*, vol. 66, no. 12, pp. 7412–7417, Dec. 2018.

[31] Y.-L. Ban, S. Yang, Z. Chen, K. Kang, and J. L.-W. Li, "Decoupled planar WWAN antennas with T-shaped protruded ground for smartphone applications," *IEEE Antennas Wireless Propag. Lett.*, vol. 13, pp. 483–486, 2014.

[32] M. Farahani, J. Pourahmadazar, M. Akbari, M. Nedil, A. R. Sebak, and T. A. Denidni, "Mutual coupling reduction in millimeter-wave MIMO antenna array using a metamaterial polarization-rotator wall," *IEEE Antennas Wireless Propag. Lett.*, vol. 16, pp. 2324–2327, 2017.

[33] M. Farahani, J. Zaid, T. A. Denidni, M. Akbari, A. R. Sebak, and M. Nedil, "Mutual coupling reduction in millimeter-wave MIMO dielectric resonator antenna using metamaterial polarization rotator wall," in *Proc. IEEE Int. Symp. Antennas Propag. & USNC/URSI Nat. Radio Sci. Meeting*, San Diego, CA, USA, Jul. 2017, pp. 1261–1262.

[34] M. Farahani, M. Akbari, M. Nedil, and T. A. Denidni, "Mutual coupling reduction in dielectric resonator MIMO antenna arrays using metasurface orthogonalize wall," in *Proc. 11th Eur. Conf. Antennas Propag. (EUCAP)*, Paris, France, Mar. 2017, pp. 985–987.

[35] M. Akbari, H. A. Ghalyon, M. Farahani, A.-R. Sebak, and T. A. Denidni "Spatially decoupling of CP antennas based on FSS for 30-GHz MIMO systems," *IEEE Access*, vol. 5, pp. 6527–6537, 2017.

[36] M. Akbari, M. M. Ali, M. Farahani, A. R. Sebak, and T. Denidni, "Spatially mutual coupling reduction between CP-MIMO antennas using FSS superstrate," *Electron. Lett.*, vol. 53, no. 8, pp. 516–518, Apr. 2017.

[37] J.-M. Hannula, T. Saarinen, J. Holopainen, and V. Viikari, "Frequency reconfigurable multiband handset antenna based on a multichannel transceiver," *IEEE Trans. Antennas Propag.*, vol. 65, no. 9, pp. 4452–4460, Sep. 2017.

[38] M. S. Sharawi, "A 5-GHz 4/8-element MIMO antenna system for IEEE 802.11AC devices," *Microw. Opt. Technol. Lett.*, vol. 55, no. 7, pp. 1589–1594, Jul. 2013.

XUGANG ZHANG was born in Henan, China, in 1994. He received the B.S. degree in communication engineering from the Central South University of Forestry and Technology, Hunan, China, in 2016. He is currently pursuing the M.S. degree in circuit and system with the School of Communication and Information Engineering, Shanghai University. His current research interests include sub-6-GHz MIMO antennas in mobile terminals and the antenna design using machine learning.

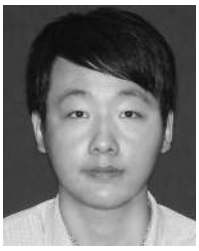

YIXIN LI was born in Hunan, China, in 1994. He received the B.S. degree from Shanghai University, Shanghai, China, in 2016, where he is currently pursuing the M.S. degree in electromagnetic field and microwave technology with the School of Communication and Information Engineering.

His current research interests include electrically small antennas, mobile terminal antennas, MIMO antennas, and 5G antennas. He is also serving as a Reviewer for IEEE Access and the *Applied Computational Electromagnetics Society Journal*.

WEI WANG was born in Ningxia, China, in 1994. He received the B.S. degree in electronic science technology from Shaoyang University, Hunan, China, in 2016. He is currently pursuing the M.S. degree in electromagnetic field and microwave technology with the School of Communication and Information Engineering, Shanghai University. His current research interest includes MIMO antennas in metal-frame smartphones.

WENHUI SHEN was born in Anhui, China, in 1972. He received the B.S. degree in electronic science technology from the Wuhan Institute of Technology, in 1994, the M.S. degree in electronic science technology from the Nanjing University of Post and Telecommunication, in 2000, and the Ph.D. degree in electrical engineering from Shanghai Jiao Tong University, in 2005.

In 1999, he was with the Nanjing Institute of Electronic Technology. From 2000 to 2002, he was an Engineer with the Shanghai Design Institute of Post and Telecommunication. He is currently an Associate Professor with Shanghai University. His research interests include microstrip antenna, smartphone antenna, genetic algorithm, and the theory of Maxwellian circuits.